Cerebral Cortex, May 2021;31: 2402–2415

doi: 10.1093/cercor/bhaa363
Advance Access Publication Date: 21 December 2020
Original Article

ORIGINAL ARTICLE

Activation of Oxytocin Receptors Excites Subicular Neurons by Multiple Signaling and Ionic Mechanisms

Binqi Hu, Cody A. Boyle and Saobo Lei

Department of Biomedical Sciences, School of Medicine and Health Sciences, University of North Dakota, Grand Forks, ND 58203, USA

Address correspondence to Saobo Lei, Department of Biomedical Sciences, School of Medicine and Health Sciences, University of North Dakota, Twamley Hall Room 201, Grand Forks, ND 58203, USA. Email: saobo.lei@und.edu.

Abstract

Oxytocin (OXT) is a nonapeptide that serves as a neuromodulator in the brain and a hormone participating in parturition and lactation in the periphery. The subiculum is the major output region of the hippocampus and an integral component in the networks that process sensory and motor cues to form a cognitive map encoding spatial, contextual, and emotional information. Whilst the subiculum expresses the highest OXT-binding sites and is the first brain region to be activated by peripheral application of OXT, the precise actions of OXT in the subiculum have not been determined. Our results demonstrate that application of the selective OXT receptor (OXTR) agonist, [Thr^4,Gly^7]-oxytocin (TGOT), excited subicular neurons via activation of TRPV1 channels, and depression of K^+ channels. The OXTR-mediated excitation of subicular neurons required the functions of phospholipase Cβ, protein kinase C, and degradation of phosphatidylinositol 4,5-bisphosphate (PIP_2). OXTR-elicited excitation of subicular neurons enhanced long-term potentiation via activation of TRPV1 channels. Our results provide a cellular and molecular mechanism to explain the physiological functions of OXT in the brain.

Key words: depolarization, K^+ channel, LTP, PKC, TRPV1

Introduction

Oxytocin (OXT) is a nonapeptide synthesized primarily by the neurosecretory cells in the paraventricular and supraoptic nuclei of the hypothalamus. In addition to the neurosecretory projections to the posterior pituitary, OXT also travels along with the axonal projections from parvocellular neurons of the hypothalamus to discrete brain regions including the hippocampus, subiculum, amygdala, and nucleus accumbens (Buijs 1978; Lang et al. 1983; Hawthorn et al. 1985). OXT functions by interacting with OXT receptors (OXTRs) or cross-activating the V_{1a} subtype of the vasopressin receptors (Song et al. 2014). Both OXTRs (Vrachnis et al. 2011) and V_{1a} receptors (Birnbaumer 2000) are coupled to $G_{q/11}$ proteins resulting in activation of phospholipase Cβ (PLCβ) which hydrolyzes PIP_2 to generate IP_3 to increase intracellular Ca^{2+} release and diacylglycerol (DAG) to activate protein kinase C (PKC). In addition to its hormonal roles in parturition and lactation, OXT is also a neuromodulator that regulates a diverse range of functions including emotional responses (Neumann 2008), social affiliation (Feldman 2012), grooming (Amico et al. 2004), sexual behaviors (Argiolas and Gessa 1991), social (Bielsky and Young 2004) and spatial (Tomizawa et al. 2003) memories, and may possess therapeutic potential for neuropsychiatric disorders, such as autism and schizophrenia (Zik and Roberts 2015). However, the cellular and molecular mechanisms whereby OXT modulates these physiological functions and neurological diseases have not been fully determined.

Whereas OXT has been shown to enhance hippocampal CA1 long-term potentiation (LTP) in vitro (Lin et al. 2012), elicit synaptic depression of previously established LTP in the dentate gyrus (DG) of anesthetized rats (Dubrovsky et al. 2002), increase the excitability of hippocampal interneurons (Muhlethaler and Dreifuss 1983; Muhlethaler et al. 1984; Zaninetti and Raggenbass 2000; Owen et al. 2013; Harden and Frazier 2016) and enhance the fidelity of spike transmission and sharpen spike timing in area CA1 (Owen et al. 2013), the subiculum expresses the

highest density of OXT-binding sites (Freund-Mercier et al. 1987; Dreifuss et al. 1989) and is the first brain region to be activated by peripheral application of OXT (Ferris et al. 2015), suggesting that the most important brain region mediating the effects of OXT is probably the subiculum. Paradoxically, the physiological functions of OXTR activation in the subiculum have not been determined, except that injection of OXT into the ventral subiculum induces penile erection (Melis et al. 2009; Melis et al. 2010; Melis and Argiolas 2011; Succu et al. 2011). In this study, we explored the effects of OXTR activation on the excitability of subicular neurons and our results demonstrate that activation of OXTRs facilitates the excitability of subicular neurons by activating TRPV1 channels and depressing a K^+ channel. Multiple signaling mechanisms including PLCβ, PKC, and PIP_2 are involved in OXTR-mediated excitation of subicular neurons. We also found that activation of OXTRs facilitates LTP at the putative CA1-subiculum synapses via activation of TRPV1 channels. Our results provide a cellular and molecular mechanism to explain the functions of OXT in vivo.

Materials and Methods

Slice Preparation

Horizontal brain slices (300 µm) were prepared from both male and female Sprague–Dawley rats (21–35 days old) purchased from Envigo RMS, INC. (Indianapolis, IN), TRPV1 knockout (KO) mice (B6.129X1-*Trpv1*^{tm1Jul}/J, strain 003770, 1–2 months), and the corresponding age-matched wild-type (WT) mice (C57BL/6 J, strain 000664) purchased from The Jackson Laboratory. The number of males and females for each experiment was kept as equal as possible. After being deeply anesthetized with isoflurane, animals were decapitated and their brains were dissected out in ice-cold saline solution that contained (in mM) 130 N-methyl-D-glucamine (NMDG)-Cl, 24 $NaHCO_3$, 3.5 KCl, 1.25 NaH_2PO_4, 2.0 $CaCl_2$, 2.0 $MgCl_2$, and 10 glucose, saturated with 95% O_2 and 5% CO_2 (pH 7.4, adjusted with HCl). Slices were then incubated in the above solution except NMDG-Cl was replaced with NaCl at 35 °C for 1 h for recovery and kept at room temperature (22–23 °C) until use. All animal procedures conformed to the guidelines approved by the University of North Dakota Animal Care and Use Committee.

Recordings of Action Potentials, Resting Membrane Potentials, and Holding Currents From Subicular Neurons

Whole-cell recordings using a Multiclamp 700B amplifier (Molecular Devices, Sunnyvale, CA) in the current- or voltage-clamp mode were made from the pyramidal neurons in the subiculum visually identified with infrared video microscopy (Olympus BX51WI) and differential interference contrast optics. During recordings, the bath temperature was routinely maintained at 33–34 °C by an in-line heater and an automatic temperature controller (TC-324C, Warner Instruments), unless stated otherwise. The recording electrodes were filled with (in mM) 112 K^+-gluconate, 8 KCl, 2 $MgCl_2$, 28 HEPES, 0.6 EGTA, 2 $ATPNa_2$, 0.4 GTPNa, and 7 phosphocreatine (pH 7.3). The extracellular solution comprised (in mM) 130 NaCl, 24 $NaHCO_3$, 3.5 KCl, 1.25 NaH_2PO4, 2.5 $CaCl_2$, 1.5 $MgCl_2$ and 10 glucose, saturated with 95% O_2 and 5% CO_2 (pH 7.4). Data were filtered at 2 kHz, digitized at 10 kHz, acquired on-line, and analyzed after-line using pCLAMP 10.7 software (Molecular Devices, Sunnyvale, CA). After the formation of whole-cell configuration, we injected currents from −100 pA to 400 pA (duration: 400 ms) at a step of 50 pA with an interval of 10 s/injection to identify the recorded neurons. Bursting cells (BCs) fire an early burst of 2–4 action potentials (APs) upon injection of depolarizing current of threshold intensity, whereas in regular firing cells (RCs), prolonged depolarization causes either a single AP or trains of single spikes (Mason 1993; Mattia et al. 1993; Hu et al. 2017). The selective OXTR agonist, [Thr^4,Gly^7]-oxytocin (TGOT) was dissolved in the extracellular solution and bath applied to the slices. To avoid potential desensitization induced by repeated applications of the agonist, one slice was limited to only one application of TGOT. Resting membrane potentials (RMPs) and holding currents (HCs) at −60 mV were recorded in the extracellular solution supplemented with tetrodotoxin (TTX, 0.5 µM), kynurenic acid (1 mM) and picrotoxin (100 µM) to block AP firing, glutamatergic, and GABAergic transmission, respectively. The capacitances of the recorded neurons were the readouts on the MultiClamp Commander Software Interface after compensation of the whole-cell capacitances. The input resistances of the neurons were obtained by linear fitting of the I-V curves constructed by injections of currents from −100 pA to +50 pA at an interval of 50 pA.

Recordings of Synaptic Currents and LTP From Subicular Pyramidal Neurons

For the recordings of AMPA EPSCs and LTP, the above-mentioned K^+-gluconate internal solution was used and the extracellular solution was supplemented with picrotoxin (100 µM) to block GABAergic transmission. The holding potential was at −60 mV and the stimulation frequency was 0.1 Hz. A stimulation electrode was placed in the alveus of the border of CA1 and subiculum to stimulate the putative CA1 input and recordings were then conducted from the neurons in the middle part of the subiculum (Wozny et al. 2008; Hu et al. 2017) (Fig. 1). An input–output curve was constructed by increasing the stimulation intensity from 50 to 400 µA with a constant stimulation duration of 0.1 ms and an interval of 50 µA. The stimulation intensity was set at which ~50% maximum AMPA EPSC amplitude was achieved. The stimulation intensity was usually between 100 and 250 µA. After recording stable basal AMPA EPSCs at −60 mV (0.1 Hz) for 5 min, TGOT (0.3 µM) or saline (0.9% NaCl) dissolved in the extracellular solution was perfused for 5 min. The maximal effect of TGOT on depolarization was usually observed within this time period. An induction protocol of high-frequency stimulation (HFS, 100 Hz for 1 s, repeated four times at an interval of 10 s, in current clamp at the RMP) was then applied to induce LTP (Wozny et al. 2008; Hu et al. 2017). Recording of AMPA EPSCs at −60 mV (0.1 Hz) was then resumed to observe the expression of LTP.

Data Analysis

Data are presented as means ± SD. TGOT concentration-response curve was fit by using the Hill equation: $I = I_{max} \times \{1/[1 + (EC_{50}/[ligand])^n]\}$, where I_{max} is the maximum response, EC_{50} is the concentration of ligand producing a half-maximal response, and n is the Hill coefficient. Because the maximal response occurred within 5 min during the application of TGOT, we measured the peak response of TGOT for statistical analysis. The control data for TGOT-induced depolarization were pooled results from the control experiments performed

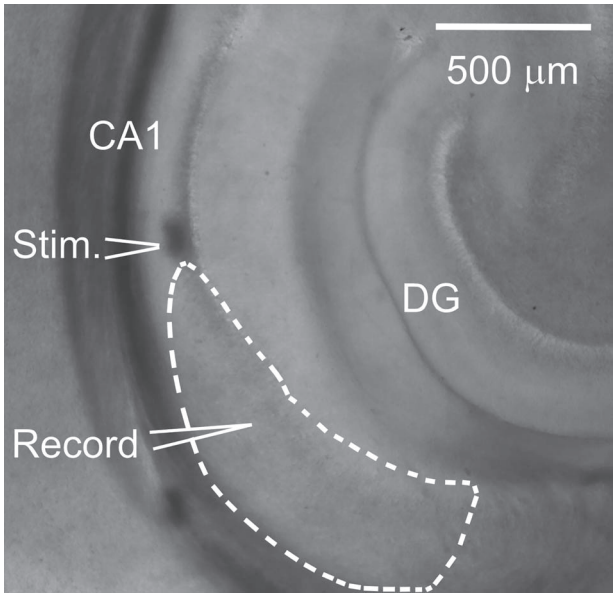

Figure 1. Graph to show the differences between CA1 and subiculum. The dashed line shows the outline of the subiculum. Stimulation electrode (denoted as Stim.) was placed in the alveus of the border of CA1 and subiculum. Recording electrode (denoted as Record) was placed in the middle of the subiculum.

for each individual pharmacological experiment. One-Way ANOVA followed by Dunnett's multiple comparison test was used for statistical analysis when the pooled control data were used for comparison. Two-Way ANOVA was used for statistical analysis of the LTPs under different conditions. Mann–Whitney test or Wilcoxon matched-pairs signed-rank test (abbreviated as Wilcoxon test in the text) was used for statistical analysis as appropriate; P values are reported throughout the text and significance was set as $P < 0.05$.

Chemicals

[Thr^4,Gly^7]-oxytocin was purchased from Bachem. The following chemicals were products of R&D systems: tetrodotoxin (TTX), kynurenic acid, picrotoxin, L-371257, GDP-β-S, U73122, U73343, heparin, thapsigargin, ryanodine, BAPTA, chelerythrine, bisindolylmaleimide II (Bis II), capsazepine, AMG9810, AMG21629, and capsaicin. Dioctanoyl phosphatidylinositol 4,5-bisphosphate (diC8-PIP$_2$) was purchased from Echelon Biosciences. URB297 was the product of MedChemExpress. Drugs were initially prepared in the stock solution, aliquoted, and stored at −20°C. For those chemicals requiring dimethyl sulfoxide (DMSO) as a solvent, the concentration of DMSO was less than 0.1%. This concentration of DMSO either in the recording pipettes or in the bath had no significant effects on neuronal activity.

Results

Activation of OXTRs Depolarizes Principal Subicular Neurons

Although the subiculum expresses the highest density of OXT-binding sites (Freund-Mercier et al. 1987; Dreifuss et al. 1989) and is the first brain region to be activated by peripheral application of OXT (Ferris et al. 2015), the effects of OXTR activation on subicular neurons remain unstudied. We determined the actions of OXTR activation on the RMPs of subicular neurons by applying the selective OXTR agonist, [Thr^4,Gly^7]-oxytocin (TGOT). Subiculum is distinguished from bordering regions by the diffuse distribution of pyramidal cells, compared to the tightly packed pyramidal cell layer of CA1, and the lack of distinct cortical layers seen in entorhinal cortex (Hu et al. 2017) (Fig. 1). Because there are two types of pyramidal neurons, that is, BCs and RCs in the subiculum according to their firing patterns (Wozny et al. 2008; Graves et al. 2012; Hu et al. 2017), we identified neuronal phenotypes by injecting negative and positive currents into the recorded cells initially (Fig. 2). BCs fire an early burst of 2–4 APs upon injection of depolarizing current of threshold intensity, whereas, in RCs, prolonged depolarization causes either a single AP or trains of single spikes (Mason 1993; Mattia et al. 1993). After identification of neuronal types, the extracellular solution was switched to one containing kynurenic acid (1 mM) to block glutamatergic transmission, picrotoxin (100 μM) to block GABAergic transmission and TTX (0.5 μM) to block APs. Under these circumstances, the effects of TGOT should arise from actions entirely at the recorded neurons. Of the 28 cells recorded, 22 cells were classified as BCs (79%) and 6 cells were categorized as RCs (21%). The ratios of BCs and RCs were generally consistent with those reported previously showing that BCs account for 75–100% of the subicular cell population (Mason 1993; Mattia et al. 1993). There was no significant difference ($P = 0.72$, Mann–Whitney test) between the capacitances of the BCs (48.3 ± 11.5 pF, $n = 22$) and that of RCs (50.0 ± 8.7 pF, $n = 6$). However, the input resistance of the BCs (61.9 ± 9.5 MΩ, $n = 22$) was significantly lower than that of the RCs (98.4 ± 28.2 MΩ, $n = 6$, $P = 0.008$, Mann–Whitney test), consistent with previous results (Greene and Mason 1996; Graves et al. 2012).

We recorded RMP responses to OXTR activation in both cell types. Bath application of TGOT (0.3 μM) for 5 min induced depolarization in both BCs (Control: -60.6 ± 2.8 mV, TGOT: -54.3 ± 4.7 mV, $n = 22$, $P < 0.0001$, Wilcoxon test, Figure 2A_1–A_3) and RCs (Control: -62.9 ± 3.4 mV, TGOT: -57.8 ± 4.1 mV, $n = 6$, $P = 0.03$, Wilcoxon test, Fig. 2B_1–B_3). There was no significant difference for TGOT-induced depolarization ($P = 0.6$, Mann–Whitney test, Fig. 2C) between BCs (6.3 ± 3.7 mV, $n = 22$) and RCs (5.2 ± 1.1 mV, $n = 6$). TGOT depolarized subicular neurons in slices cut from both male (Control: -60.9 ± 3.1 mV, TGOT: -54.7 ± 5.2 mV, $n = 16$, $P < 0.0001$, Wilcoxon test) and female (Control: -61.3 ± 2.9 mV, TGOT: -55.5 ± 4.5 mV, $n = 12$, $P = 0.0005$, Wilcoxon test) rats. There was no significant difference ($P = 0.8$, Mann–Whitney test) for TGOT-mediated net depolarization in slices cut from male (6.2 ± 3.9 mV, $n = 16$) and female (5.8 ± 2.4 mV, $n = 12$) rats. The EC$_{50}$ of TGOT was calculated to be 58 nM (Fig. 2D). We, therefore, used TGOT at 0.3 μM and recorded from both BCs and RCs in slices cut from both male and female rats for the remaining experiments. The effect of TGOT was mediated by activation of OXTRs because pretreatment of slices with and continuous bath application of the selective OXTR antagonist, L-371257 (3 μM) (Pettibone et al. 1995), blocked TGOT-induced depolarization (L-371257: -61.0 ± 3.2 mV, L-371257 + TGOT: -60.2 ± 4.0 mV, $n = 8$, $P = 0.46$, Wilcoxon test; net depolarization: 0.78 ± 1.88 mV, $P < 0.001$ versus TGOT alone, One-Way ANOVA followed by Dunnett's test, Fig. 2E_1–E_2). Activation of OXTRs induced an inward current in voltage-clamp at −60 mV (-26.5 ± 14.8 pA, $n = 30$, $P < 0.0001$, Wilcoxon test, Fig. 2F_1–F_2). There was no significant difference ($P = 0.66$, Mann–Whitney test) for TGOT-induced inward currents between BCs (-25.7 ± 15.0 pA, $n = 23$, $P < 0.0001$, Wilcoxon test) and RCs (-29.3 ± 14.9 pA, $n = 7$, $P = 0.016$, Wilcoxon test).

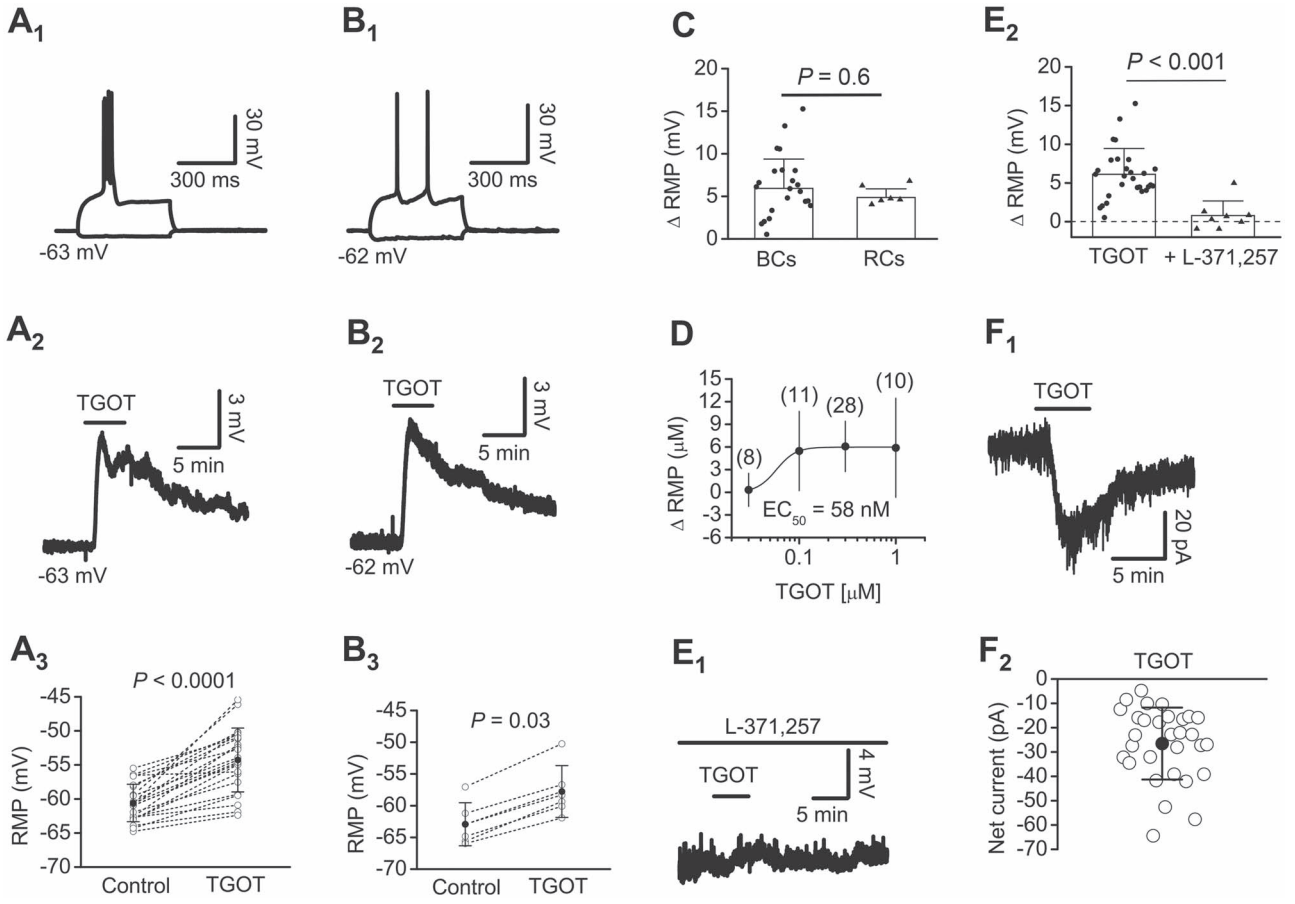

Figure 2. Activation of OXTRs depolarizes both BCs and RCs in the subiculum. (A_1–A_3) Bath application of the OXTR agonist, TGOT (0.3 μM) depolarized subicular BCs. (A_1) Voltage responses elicited by injecting a negative (−50 pA) and a positive (+100 pA) current. Note the bursting response elicited by the positive current, demonstrating it was a BC. (A_2) Depolarization elicited by bath application of TGOT from the same BC. (A_3) Summary graph showing TGOT-induced depolarization in BCs ($n = 22$). (B_1–B_3) Bath application of TGOT (0.3 μM) depolarized subicular RCs. (B_1) Voltage responses elicited by injecting a negative (−50 pA) and a positive (+100 pA) current. Note the single and regular spikes elicited by the positive current, demonstrating it was a RC. (B_2) Depolarization elicited by bath application of TGOT from the same RC. (B_3) Summary graph showing TGOT-induced depolarization in RCs ($n = 6$). (*C*) There was no significant difference for TGOT-elicited net depolarization between BCs and RCs. (*D*) Concentration-response curve of TGOT-elicited depolarization. The numbers in the parentheses are the numbers of cells used. (E_1–E_2) Treatment of slices with the selective OXTR antagonist, L-371257 (3 μM), blocked TGOT-elicited depolarization. (E_1) RMP recorded from a subicular neuron prior to, during and after the application of TGOT in the continuous presence of L-371257. (E_2) Summary graph showing the comparison of the depolarization induced by TGOT alone and that elicited by TGOT in the continuous presence of L-371257. (F_1–F_2) Application of TGOT induced an inward current in subicular neurons. (F_1) Holding current recorded at −60 mV from a subicular neuron before, during and after the application of TGOT. (F_2) Summary graph showing the net inward current elicited by TGOT ($n = 30$).

OXTR-Mediated Depolarization Requires the Functions of G PROTEINS, PLCβ and PKC but is Independent of Intracellular Ca^{2+} Release

Because OXTRs are coupled to $G\alpha_{q/11}$, we next examined the roles of G proteins in OXTR-induced depolarization. Intracellular application of the G protein inactivator, GDP-β-S (0.5 mM), via the recording pipettes significantly reduced TGOT-induced depolarization (Control: −62.5 ± 6.6 mV, TGOT: −61.5 ± 7.3 mV, net depolarization: 0.97 ± 1.20 mV, $n = 13$, $P = 0.013$, Wilcoxon test; $P < 0.0001$ vs. TGOT alone, One-Way ANOVA followed by Dunnett's test, Fig. 3A and *H*), demonstrating that G proteins are required for OXTR-induced depolarization of subicular neurons. Activation of OXTRs increases the function of PLCβ resulting in the hydrolysis of PIP_2 to generate IP_3 to increase intracellular Ca^{2+} release and DAG to activate PKC. We next examined the roles of this pathway in OXTR-induced depolarization. Slices were pretreated with the selective PLCβ inhibitor, U73122 (5 μM), for > 2 h. The same concentration of the inactive analog U73343 was used as a control. Under these circumstances, application of TGOT induced a significantly smaller depolarization in the slices treated with U73122 (Control: −58.5 ± 4.5 mV, TGOT: −56.4 ± 4.9 mV, net depolarization: 2.0 ± 1.4 mV, $n = 17$, $P = 0.0002$, Wilcoxon test, Fig. 3B and *H*), compared with the slices treated with U73343 (Control: −62.4 ± 3.1 mV, TGOT: −53.9 ± 6.5 mV, net depolarization: 8.5 ± 5.1 mV, $P < 0.001$, Wilcoxon test; $P < 0.001$ vs. U73122, Mann–Whitney test, Fig. 3C and *H*). These results demonstrate that the function of PLCβ is required for OXTR-elicited excitation of subicular neurons.

We tested the roles of intracellular Ca^{2+} release in OXTR-elicited depolarization. Application of the IP_3 receptor inhibitor, heparin (2 mg/ml), via the recording pipettes, failed to significantly alter TGOT-induced depolarization (Control: −62.2 ± 4.0 mV, TGOT: −56.7 ± 4.7 mV, net depolarization: 5.5 ± 2.2 mV, $n = 10$, $P = 0.002$, Wilcoxon test; $P > 0.05$, vs. TGOT alone, One-Way ANOVA followed by Dunnett's test, Fig. 3D and *H*), demonstrating that IP_3 receptors are not required for TGOT-induced depolarization. Likewise, intracellular application of the sarco-endoplasmic reticulum Ca^{2+}-ATPase inhibitor, thapsigargin

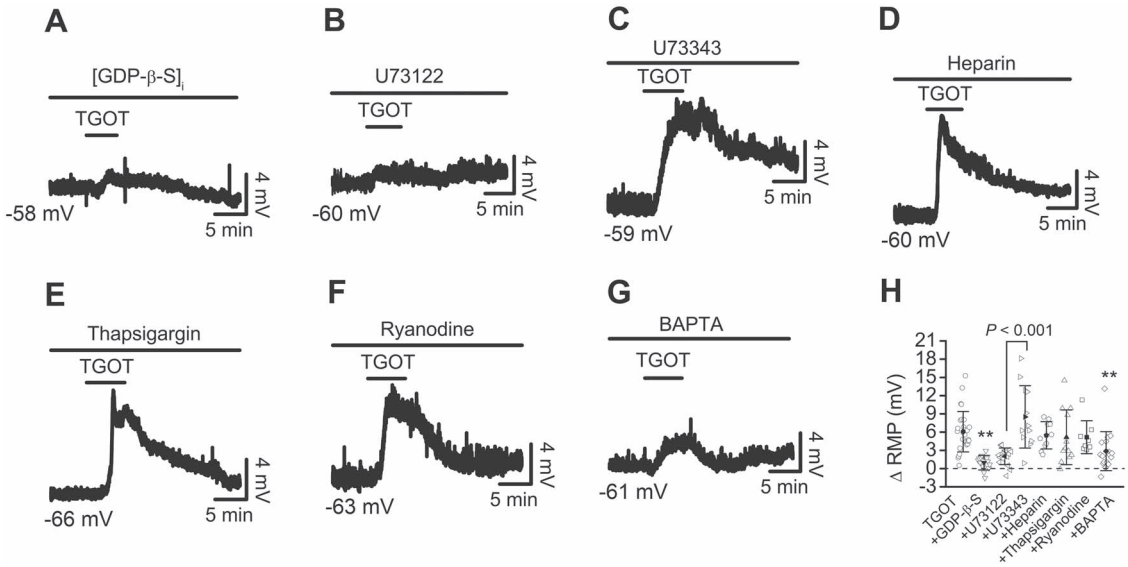

Figure 3. OXTR-mediated depolarization of subicular neurons requires the functions of G proteins and PLCβ, but is independent of intracellular Ca^{2+}release. (*A*) Intracellular perfusion of GDP-β-S (0.5 mM) inhibited TGOT-induced depolarization recorded from a subicular neuron. (*B*) Pretreatment of slices with U73122 (5 μM) depressed TGOT-induced depolarization. (*C*) Pretreatment of slices with the inactive analog, U73343 (5 μM), in the same fashion did not block TGOT-elicited depolarization. (*D*) Intracellular perfusion of heparin (2 mg/ml) to block IP_3 receptors did not block TGOT-induced depolarization. (*E*) Intracellular dialysis of the sarco-endoplasmic reticulum Ca^{2+}-ATPase inhibitor, thapsigargin (10 μM), failed to block TGOT-elicited depolarization. (*F*) Intracellular application of ryanodine (100 μM) to block ryanodine receptors had no effect on TGOT-evoked depolarization. (*G*) Dialysis of BAPTA (10 mM) via the recording pipettes attenuated TGOT-elicited depolarization. (*H*) Summary graph. $^{**}P < 0.01$ versus TGOT alone.

(10 μM), via the recording pipettes did not significantly change TGOT-mediated depolarization (Control: -63.7 ± 1.8 mV, TGOT: -58.6 ± 5.5 mV, net depolarization: 5.1 ± 4.5 mV, $n = 12$, $P = 0.001$, Wilcoxon test; $P > 0.05$ vs. TGOT alone, One-Way ANOVA followed by Dunnett's test, Fig. 3*E* and *H*). We also probed a potential role of Ca^{2+} released from ryanodine-sensitive stores by intracellular dialysis of ryanodine at 100 μM to inhibit the ryanodine receptors. Application of ryanodine did not significantly alter TGOT-elicited depolarization (Control: -58.4 ± 2.0 mV, TGOT: -53.2 ± 3.6 mV, net depolarization: 5.2 ± 2.7 mV, $n = 8$, $P = 0.008$, Wilcoxon test; $P > 0.05$ vs. TGOT alone, One-Way ANOVA followed by Dunnett's Test, Fig. 3*F* and *H*). These results demonstrate that intracellular Ca^{2+} release is not required for TGOT-induced depolarization. However, dialysis of BAPTA (10 mM) via the recording pipettes to chelate intracellular Ca^{2+} significantly reduced OXTR-elicited depolarization (Control: -62.4 ± 3.7 mV, TGOT: -59.5 ± 5.8 mV, net depolarization: 2.9 ± 3.2 mV, $n = 17$, $P < 0.001$, Wilcoxon test; $P < 0.01$ vs. TGOT alone, One-Way ANOVA followed by Dunnett's Test, Fig. 3*G–H*). One explanation for these results is that OXTR-induced depolarization is not triggered by Ca^{2+} released from individual Ca^{2+} stores. However, BAPTA lowered the basal intracellular Ca^{2+} level, which may be required for the functions of Ca^{2+}-dependent signaling molecules.

We further tested the roles of PKC in TGOT-mediated excitation of subicular neurons. Slices were pretreated with the selective PKC inhibitor, chelerythrine (10 μM), for >2 h, and the extracellular solution continuously contained the same concentration of chelerythrine. Treatment of slices with chelerythrine significantly reduced TGOT-induced depolarization (chelerythrine: -62.5 ± 2.7 mV, chelerythrine + TGOT: -61.0 ± 3.9 mV, net depolarization: 1.5 ± 2.1 mV, $n = 15$, $P = 0.022$, Wilcoxon test; $P < 0.0001$ vs. TGOT alone, One-Way ANOVA followed by Dunnett's test, Fig. 4*A* and *D*). Furthermore, pretreatment of slices with and continuous bath application of bisindolylmaleimide II (Bis II, 1 μM), another PKC inhibitor, significantly reduced OXTR-elicited depolarization (Bis II: -61.6 ± 2.9 mV, Bis II + TGOT: -58.2 ± 3.2 mV, net depolarization: 3.4 ± 2.2 mV, $n = 16$, $P < 0.0001$, Wilcoxon test; $P < 0.05$ vs. TGOT alone, One-Way ANOVA followed by Dunnett's test, Fig. 4*B* and *D*). These results together indicate that PKC is required for OXTR-mediated depolarization of subicular neurons.

Depletion of PIP_2 is Involved in OXTR-Elicited Depolarization of Subicular Neurons

Because PLCβ-mediated depletion of PIP_2 has been demonstrated to be a mechanism underlying the modulation of numerous ion channels (Suh and Hille 2008; Rodriguez-Menchaca et al. 2012), we also probed the roles of PIP_2 depletion induced by activation of PLCβ in response to OXTR activation. Inclusion of the short-chain, water-soluble analog dioctanoyl (diC8)-PIP_2 (20 μM) in the recording pipettes significantly reduced TGOT-evoked depolarization (Control: -60.5 ± 2.4 mV, TGOT: -58.5 ± 3.1 mV, net depolarization: 1.9 ± 2.9 mV, $n = 13$, $P = 0.04$, Wilcoxon test; $P < 0.0001$ vs. TGOT alone, One-Way ANOVA followed by Dunnett's test, Fig. 4*C–D*), demonstrating that depletion of PIP_2 is involved in OXTR-mediated depolarization of subicular neurons.

OXTR-Elicited Depolarization is Mediated by Activation of Cation Channels and Depression of K^+ Channels

We then probed the ionic mechanisms underlying OXTR-induced depolarization by constructing the current-voltage (I-V) relationship for the currents evoked by TGOT. The extracellular solution contained TTX (0.5 μM) to block voltage-gated Na^+ channels. Cells were held at −60 mV and stepped from −140 to −40 mV for 400 ms at a voltage interval of 10 mV every 10 s. Steady-state currents were measured within 5 ms prior to the

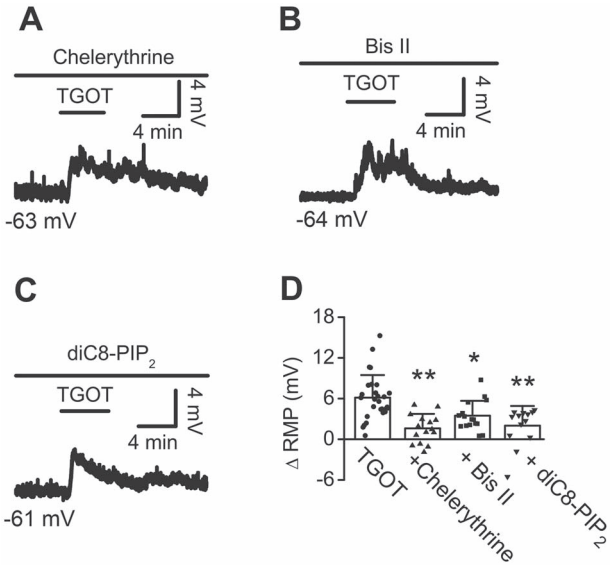

Figure 4. PKC and depletion of PIP_2 are involved in OXTR-mediated depolarization of subicular neurons. (*A*) Bath application of TGOT induced a smaller depolarization in a slice pretreated with the selective PKC inhibitor, chelerythrine (10 μM). (*B*) Bath application of TGOT elicited a smaller depolarization in a slice pretreated with the selective PKC inhibitor, Bis II (1 μM). (*C*) Intracellular perfusion of diC8-PIP_2 (20 μM) reduced TGOT-evoked depolarization. (*D*) Summary graph. $^*P < 0.05$, $^{**}P < 0.01$ versus TGOT alone.

end of the voltage-step protocol. Under these circumstances, there was no significant difference for the I-V curve during perfusion with the extracellular solution for 5 min (Fig. 5A_1–A_3), demonstrating that the I-V curve is stable for at least 5 min. For each cell, after recording the control I-V curve, the bath was perfused with the same extracellular solution containing TGOT. The holding current was recorded during the application of TGOT to discern the maximal effect of TGOT. I-V curve was recorded again when the peak response of TGOT was observed. Out of the 16 cells recorded, 12 cells (~75%) showed an I-V curve of cationic channels, that is, TGOT persistently induced an inward current between −140 and − 40 mV (Fig. 5B_1–B_3), demonstrating that OXTR activation depolarizes subicular neurons by activating a cationic conductance. The remaining 4 cells (~25%) displayed an I-V curve of a K^+ channel with a reversal potential of −97.0 ± 11.2 mV ($n = 4$, Fig. 5C_1–C_3), suggesting that activation of OXTRs depolarizes a small population of subicular neurons by depression of K^+ conductance.

We then performed another set of experiments to measure the reversal potential of the TGOT-elicited cationic currents by extending to more positive voltages. The extracellular solution contained TTX (0.5 μM) to block voltage-gated Na^+ channels and $CdCl_2$ (200 μM) and $NiCl_2$ (1 mM) to inhibit voltage-gated Ca^{2+} channels. Under these circumstances, the application of TGOT elicited a cationic current of outward rectification with a reversal potential of −25.5 ± 22.9 mV ($n = 10$, Fig. 5D_1–D_3), further confirming a predominant role of cationic channels in OXTR-mediated depolarization.

TRPV1 Channels are Involved in OXTR-Mediated Excitation of Subicular Neurons

The I-V relationship of TGOT-sensitive cationic currents displayed outward rectification, resembling that of TRPV1 channels (Wu et al. 2010). Because TRPV1 channels are sensitive to temperature and the recording temperature in the current study was at 33–34 °C, we examined the effects of TGOT-induced depolarization at room temperature. Bath application of TGOT induced a significantly smaller depolarization when recordings were performed at room temperature (22–23 °C) (Control: −58.8 ± 3.1 mV, TGOT: −55.5 ± 3.5 mV, net depolarization: 3.3 ± 1.9 mV, $n = 21$, $P < 0.0001$, Wilcoxon test; $P < 0.01$ vs. TGOT-induced depolarization at 33 °C, One-Way ANOVA followed by Dunnett's test, Fig. 6*A* and *G*). We further probed the roles of TRPV1 channels in TGOT-mediated excitation of subicular neurons by application of the selective TRPV1 blockers. Application of capsazepine (10 μM), a selective TRPV1 blocker, significantly reduced TGOT-elicited depolarization (Capsazepine: −64.4 ± 7.5 mV, Capsazepine + TGOT: −61.4 ± 8.1 mV, net depolarization: 3.0 ± 1.9 mV, $n = 17$, $P < 0.0001$, Wilcoxon test; $P < 0.01$ vs. TGOT alone, One-Way ANOVA followed by Dunnett's test, Fig. 6*B* and *G*). Moreover, TGOT-induced depolarization was significantly reduced by bath applications of other two selective TRPV1 blockers, AMG9810 (10 μM, Control: −63.6 ± 3.1 mV, TGOT: −60.2 ± 3.7 mV, $P = 0.0005$, Wilcoxon test; $P < 0.05$ vs. TGOT alone, One-Way ANOVA followed by Dunnett's test, Fig. 6*C* and *G*) and AMG21629 (3 μM, Control: −62.4 ± 2.0 mV, TGOT: −58.9 ± 2.8 mV, net depolarization: 3.4 ± 1.2 mV, $n = 10$, $P = 0.002$, Wilcoxon test; $P < 0.05$ vs. TGOT alone, One-Way ANOVA followed by Dunnett's test, Fig. 6*D* and *G*). These results suggest that OXTR activation depolarizes subicular neurons by activating TRPV1 channels.

If TRPV1 channels are involved in TGOT-elicited depolarization, application of the selective TRPV1 agonist, capsaicin should depolarize subicular neurons. Consistent with our speculation, bath application of capsaicin (50 μM) elicited significant depolarization in the subicular neurons (Control: −59.9 ± 2.6 mV, capsaicin: −56.6 ± 4.3 mV, net depolarization: 3.2 ± 3.0 mV, $n = 11$, $P = 0.001$, Wilcoxon test, Fig. 6*E* and *G*). Pretreatment of slices with and continuous bath application of the selective TRPV1 channel blocker, capsazepine (10 μM), blocked capsaicin-induced depolarization (Capsazepine: −60.6 ± 2.1 mV, Capsazepine + Capsaicin: −60.7 ± 2.4 mV, net depolarization: −0.07 ± 0.78 mV, $n = 8$, $P = 0.84$, Wilcoxon test; $P < 0.001$ vs. Capsaicin alone, Mann–Whitney test, Fig. 6*F*–*G*), further confirming that activation of TRPV1 channels depolarizes subicular neurons.

We then utilized TRPV1 KO mice to further confirm the pharmacological experiments. Application of TGOT elicited a significantly smaller depolarization in slices cut from TRPV1 KO mice (Control: −60.6 ± 2.6 mV, TGOT: −58.6 ± 3.9 mV, net depolarization: 1.9 ± 2.7 mV, $n = 23$ cells from 4 mice, $P = 0.0007$, Wilcoxon test; Fig. 6*H* and *J*), compared with TGOT-induced depolarization in slices cut from WT mice (Control: −60.4 ± 3.4 mV, TGOT: −54.2 ± 5.4 mV, net depolarization: 6.2 ± 4.3 mV, $n = 15$ cells from 3 mice, $P < 0.0001$, Wilcoxon test; $P = 0.0002$, vs TRPV1 KO mice, Mann–Whitney test, Fig. 6*I*–*J*). These data together demonstrate that activation of TRPV1 channels is a mechanism responsible for OXTR-mediated excitation of subicular neurons.

In addition to being activated by capsaicin, TRPV1 channels are also activated by the endocannabinoid, anandamide (Smart et al. 2000; Fenwick et al. 2017; Muller et al. 2018). Because activation of OXTRs in the nucleus accumbens increases the mobilization of anandamide to mediate the prosocial effect of OXT (Wei et al. 2015), we tested a hypothesis that activation of OXTRs increases the production or mobilization of anandamide which then activates TRPV1 channels, leading to excitation of subicular neurons. To test this hypothesis, we first tested whether the

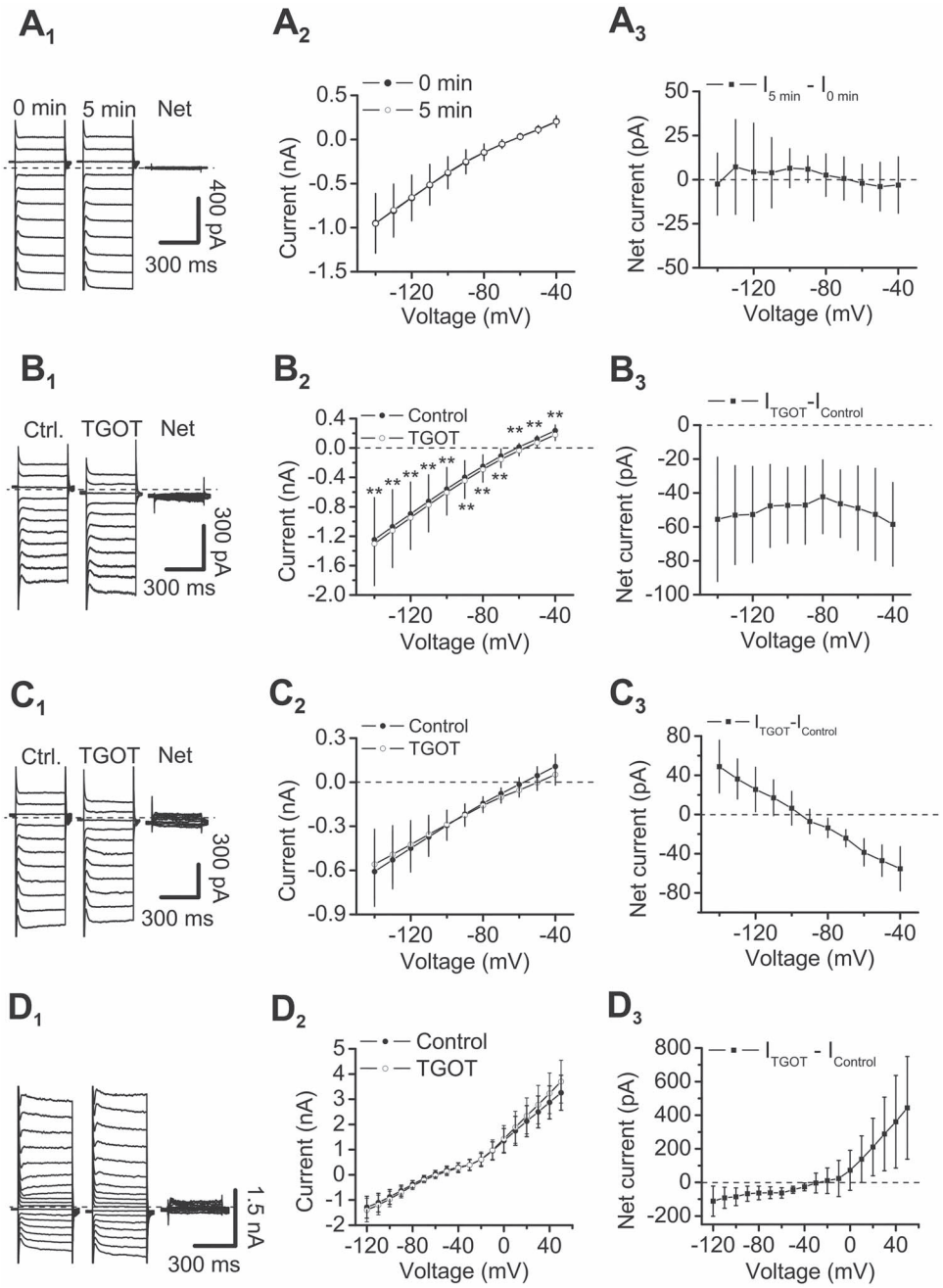

Figure 5. Activation of OXTRs depolarizes subicular neurons by activating a cationic conductance and depressing a K^+ conductance. (A_1-A_3) After the holding currents at −60 mV were stable, perfusion of the extracellular solution for 5 min did not alter I-V curve. A_1, Currents recorded from a subicular neuron elicited by the voltage-step protocol before (left) and during (middle) the perfusion of extracellular solution for 5 min and the net current obtained by subtraction (right). The dashed line represents the current at 0 pA. (A_2) I-V curves of the currents elicited by the voltage-step protocol before and during the perfusion of extracellular solution for 5 min ($n = 9$, $P > 0.05$ at each voltage, Wilcoxon test). (A_3) Net currents obtained by subtracting the currents in control condition from those recorded from the same cells during the perfusion of extracellular solution for 5 min. (B_1–B_3) TGOT depolarized subicular neurons predominantly by activating a cationic conductance. (B_1) Currents recorded from a subicular neuron in response to the voltage-step protocol before (left) and during (middle) the application of TGOT and the net current obtained by subtraction (right). (B_2) I-V curves of the currents elicited by the voltage-step protocol before and during the application of TGOT ($n = 12$, $^{**}P < 0.01$, Wilcoxon test). (B_3) Net currents obtained by subtracting the currents in control condition from those recorded from the same cells during the application of TGOT. (C_1–C_3) Application of TGOT excited a subpopulation of subicular neurons by depressing a K^+ conductance. (C_1) Currents recorded from a subicular neuron in response to the voltage-step protocol before (left) and during (middle) the application of TGOT and the net current obtained by subtraction (right). (C_2) I-V curves of the currents elicited by the voltage-step protocol before and during the application of TGOT ($n = 4$). (C_3) Net currents obtained by subtracting the currents in control condition from those recorded from the same cells during the application of TGOT. (D_1–D_3) TGOT elicited a cationic channel current with a reversal potential of about −25 mV. The extracellular solution was supplemented with $CdCl_2$ (200 μM) and $NiCl_2$ (1 mM) to block voltage-gated Ca^{2+} channels and TTX (0.5 μM) to block voltage-gated Na^+ channels. (D_1) Current traces evoked by a voltage step protocol (from −120 mV to +50 mV for 400 ms at a voltage interval of 10 mV every 10 s) before (left) and during (middle) the application of TGOT, and the net current obtained by subtraction (right). Steady-state currents were measured within 5 ms prior to the end of the step voltage protocols. (D_2) I-V curves of the currents elicited by the voltage-step protocol before and during the application of TGOT ($n = 10$). (D_3) Net currents obtained by subtracting the currents in the control condition from those recorded from the same cells during the application of TGOT ($n = 10$).

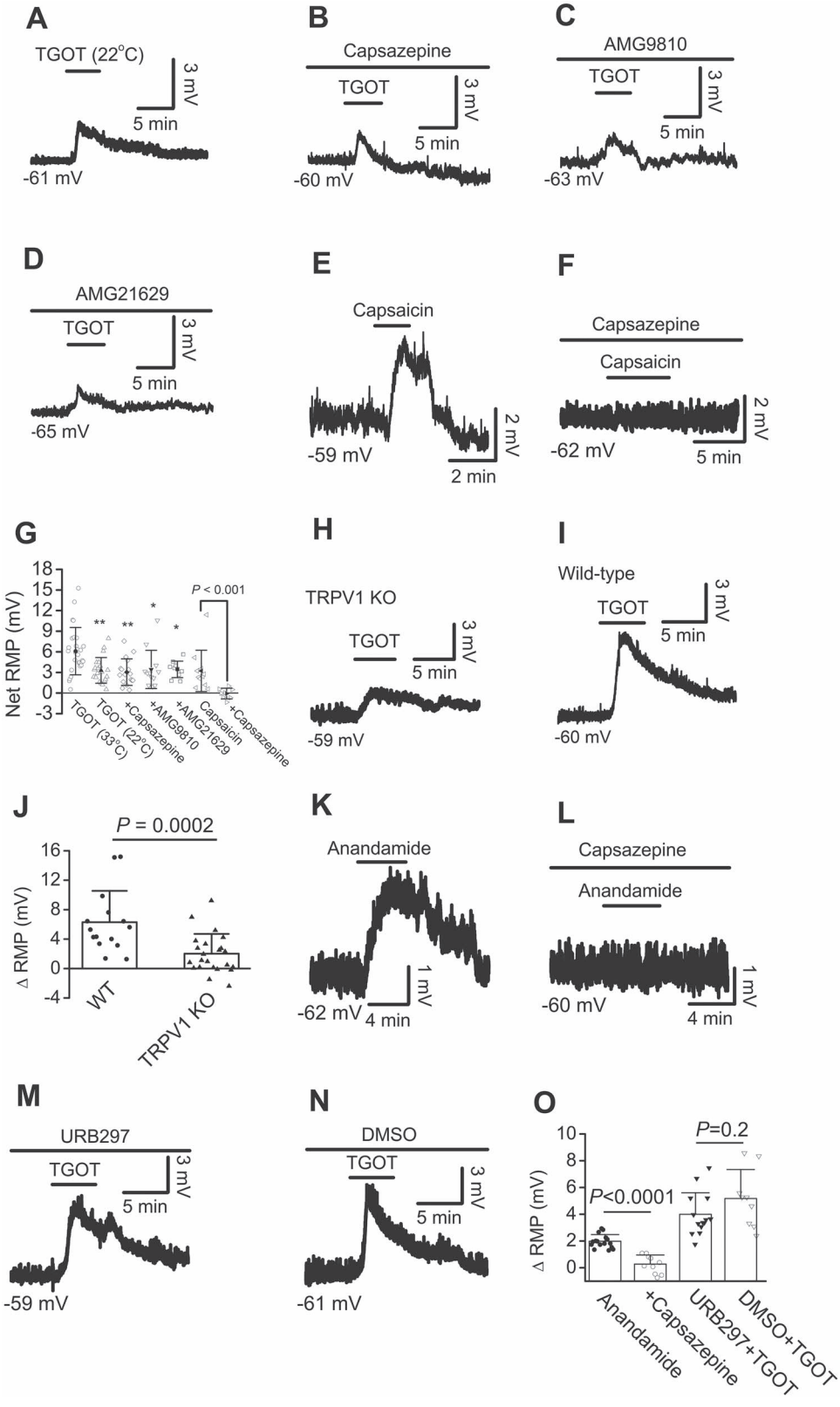

Figure 6. TRPV1 channels are involved in OXTR-elicited depolarization of subicular neurons. (*A*) Bath application of TGOT induced a smaller depolarization when the recording was performed at room temperature (22 °C). As described in Materials and Methods, all other experiments except this one were performed by warming the extracellular solution to 33°C. (*B*) Application of TGOT induced a smaller depolarization in a slice treated with the selective TRPV1 blocker, capsazepine (10 μM). (*C*) Application of TGOT induced a smaller depolarization in a slice treated with the selective TRPV1 blocker, AMG9810 (10 μM). (*D*) Application of TGOT induced a smaller depolarization in a slice treated with the selective TRPV1 blocker, AMG21629 (3 μM). (*E*) Bath application of the selective TRPV1 channel activator, capsaicin

application of anandamide depolarizes subicular neurons. Bath application of anandamide (50 μM) depolarized subicular neurons (Control: −61.0 ± 2.5 mV, Anandamide: −59.2 ± 2.6 mV, net depolarization: 1.8 ± 0.7 mV, $n = 16$, $P < 0.0001$, Wilcoxon test, Fig. 6K and O) in the extracellular solution containing AM251 (10 μM), the selective antagonist/inverse agonist of CB1 receptors which are the major cannabinoid receptors expressed on brain neurons. Pretreatment of slices with and continuous bath application of the selective TRPV1 channel blocker, capsazepine (10 μM), blocked anandamide-induced depolarization (Capsazepine: −60.9 ± 2.3 mV, Capasazepine + Anandamide: −60.6 ± 2.1 mV, net depolarization: 0.3 ± 0.7 mV, $n = 10$, $P = 0.28$, Wilcoxon test, Fig. 6L and O), indicating that anandamide-elicited depolarization is mediated by activation of TRPV1 channels. To test the potential role of endogenous anandamide in OXTR-mediated depolarization, we applied URB297, the selective inhibitor for fatty acid amidohydrolase (FAAH) which is responsible for the hydrolysis of anandamide. The rationale is that inhibition of FAAH would decrease the degradation of anandamide and augment TGOT-elicited depolarization. However, treatment of slices with URB97 (1 μM) failed to alter significantly TGOT-induced depolarization (URB297: −61.6 ± 2.2 mV, URB297 + TGOT: −57.7 ± 2.8 mV, net depolarization: 4.0 ± 1.6 mV, $n = 14$, $P = 0.0001$, Wilcoxon test, Fig. 6M and O), compared with the slices treated with vehicle (DMSO) in the same fashion (DMSO: −62.3 ± 4.5 mV, DMSO + TGOT: −57.1 ± 3.6 mV, net depolarization: 5.2 ± 2.2 mV, $n = 9$, $P = 0.004$, Wilcoxon test; $P = 0.2$ vs. data treated with URB297, Mann–Whitney test, Fig. 6N–O). These results demonstrate that anandamide is unlikely to be a mediator responsible for OXTR-mediated depolarization.

Activation of OXTRs Induces AP Firing or Subthreshold Depolarization of Subicular Neurons

We further tested the roles of OXTR activation on neuronal excitability in the subiculum. The extracellular solution contained kynurenic acid (1 mM) and picrotoxin (100 μM) to block synaptic transmission and the intracellular solution was the K^+-gluconate-containing internal solution. Under these circumstances, application of TGOT induced AP firing in 16 cells out of the 31 cells (52%) recorded (283 ± 227 APs/min, $n = 16$, $P < 0.0001$, Wilcoxon test, Fig. 7A_1–A_2). The remaining 15 cells (48%) displayed only subthreshold depolarization (Control: −62.5 ± 3.7 mV, TGOT: −58.8 ± 3.6 mV, $n = 15$, $P < 0.0001$, Wilcoxon test, Fig. 7B_1–B_2).

Activation of OXTRs Facilitates LTP at the CA1-Subiculum Synapses via Postsynaptic Depolarization

Because the subiculum is the principal target of CA1 pyramidal neurons, we examined a potential role of OXTR activation on synaptic transmission and plasticity at the putative CA1-subiculum synapses by recording AMPA EPSCs from the subiculum evoked via Alvear stimulation (Wozny et al. 2008; Hu et al. 2017) (Fig. 1). The extracellular solution contained picrotoxin (100 μM) to block the GABAergic response. Under these circumstances, application of TGOT did not alter significantly AMPA EPSC amplitude (86 ± 21% of control, $n = 8$, $P = 0.25$, Wilcoxon test, Fig. 8A and B), demonstrating that OXTR activation does not modulate basal glutamatergic transmission in the subiculum, congruous with the result showing that activation of OXTRs does not modulate basal glutamatergic transmission in the CA1 region (Tomizawa et al. 2003). Because activation of OXTRs in the CA1 region enhances LTP (Tomizawa et al. 2003; Lin et al. 2012), we then examined the effects of OXTR activation on LTP at the putative CA1-subiculum synapses. After recording stable basal EPSCs for 5 min, TGOT or saline (0.9% NaCl, used to prepare TGOT stock solution) dissolved in the extracellular solution was perfused for 5 min because the maximal effect of TGOT was observed within this period. An induction protocol of high-frequency stimulation (HFS, 100 Hz for 1 s, repeated 4 times at an interval of 10 s, in current-clamp at the RMP) (Wozny et al. 2008; Hu et al. 2017) was then applied to induce LTP. Compared with the LTP induced in slices treated with saline (173 ± 37% of control, $n = 12$, $P = 0.0005$ vs. baseline, Wilcoxon test, Fig. 8C and F), application of TGOT significantly ($F_{(1,25)} = 12.41$, $P = 0.002$) increased LTP (308 ± 156% of control, $n = 15$, $P < 0.0001$ vs. baseline, Wilcoxon test, Fig. 8D and F), demonstrating that activation of OXTRs facilitates LTP.

We further tested whether OXTR-mediated depolarization of subicular neurons is required for its facilitation of LTP. After recording stable basal AMPA EPSCs for 5 min, TGOT dissolved in the extracellular solution was perfused for ~5 min to observe the maximal depolarizing effect of TGOT. We then injected a negative current at the end of TGOT application to bring the membrane potential back to the initial level (hyperpolarization) during the application of the induction protocol. Under these circumstances, there was no significant difference ($F_{(1,20)} = 3.57$, $P = 0.073$) for the magnitude of LTP between the slices treated with TGOT but injected with a negative current (194 ± 48% of control, $n = 10$, $P = 0.002$ vs. baseline, Wilcoxon test, Fig. 8E and F) and the slices treated with saline. The magnitude of LTP after treatment of TGOT followed by negative current injection was significantly smaller ($F_{(1,23)} = 7.17$, $P = 0.014$), compared with the LTP after treatment with TGOT alone (Fig. 8F). These results together demonstrate that OXTR-mediated depolarization is required for TGOT-induced facilitation of LTP.

OXTR-Elicited Augmentation of LTP Requires the Function of TRPV1 Channels

Because TRPV1 channels are involved in OXTR-elicited depolarization, we tested the roles of TRPV1 channels in OXTR-induced augmentation of LTP by using the TRPV1 KO mice. Application of the induction protocol concomitantly with the perfusion of TGOT significantly increased LTP in the slices cut from WT mice ($F_{(1,23)} = 12.85$, $P = 0.002$, Fig. 8G). However, the application of TGOT failed to significantly increase LTP in slices

(50 μM), depolarized a subicular neuron. (F) Bath application of the TRPV1 blocker, capsazepine (10 μM), blocked capsaicin-induced depolarization. (G) Summary graph. $^{**}P < 0.01$, $^{*}P < 0.05$ versus TGOT-induced depolarization at 33 °C (One-Way ANOVA followed by Dunnett's test). (H) TGOT induced a smaller depolarization in a slice cut from a TRPV1 KO mouse. (I) Depolarization evoked by TGOT recorded from a subicular neuron in a slice cut from a WT mouse. (J) Summary graph. (K) Bath application of anandamide (50 μM) depolarized a subicular neuron. (L) Bath application of the TRPV1 blocker, capsazepine (10 μM), blocked anandamide-elicited depolarization. (M) Prior treatment of slices with and continuous bath application of URB297 (1 μM) did not augment TGOT-induced depolarization. (N) Application of TGOT induced a comparable depolarization in slices treated with the vehicle, DMSO. (O), Summary graph.

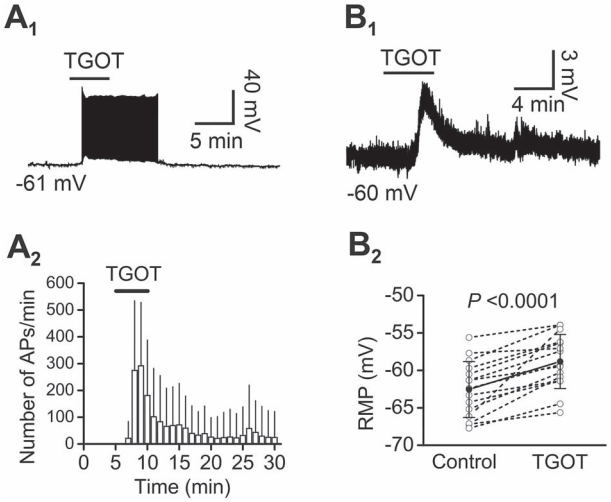

Figure 7. Activation of OXTRs induces AP firing or subthreshold depolarization in subicular neurons. (A_1–A_2) Bath application of TGOT induced AP firing in a subpopulation of subicular neurons. (A_1) AP firing recorded from a subicular neuron in response to bath application of TGOT. (A_2) Time course of TGOT-induced AP firing pooled from 16 subicular neurons. (B_1–B_2) Bath application of TGOT elicited subthreshold depolarization in a subpopulation of subicular neurons. (B_1) Subthreshold depolarization recorded from a subicular neuron in response to bath application of TGOT. (B_2) RMPs recorded from 15 subicular neurons before and during the application of TGOT.

cut from TRPV1 KO mice ($F_{(1,21)} = 0.06$, $P = 0.81$, Fig. 8*H*), demonstrating that TRPV1 channels are required for OXTR-mediated facilitation of LTP at the putative CA1-subiculum synapses.

Discussion

Our results demonstrate that activation of OXTRs excites subicular neurons predominantly by activating TRPV1 channels, although OXTR activation depolarizes about one-fourth population of subicular neurons via inhibition of K^+ channels. OXTR-elicited excitation of subicular neurons is dependent on PLCβ and involves PKC and depletion of PIP_2. OXTR-elicited depolarization facilitates LTP at the putative CA1-subiculum synapses via activation of TRPV1 channels. Our results provide a cellular and molecular mechanism whereby activation of OXTRs facilitates neuronal network activity.

We have shown that activation of OXTRs facilitates neuronal excitability in ~75% of subicular neurons by activating TRPV1 channels. The I-V curve of the TGOT-induced currents showed outward rectification, resembling that of the TRPV1 channels. Application of three selective TRPV1 blockers significantly reduced OXTR-elicited depolarization and application of TGOT evoked a significantly smaller depolarization in slices cut from TRPV1 KO mice compared with the TGOT-elicited depolarization recorded from the subicular neurons in the slices cut from WT mice. All these results together demonstrate that TRPV1 channels are the primary channels responsible for OXTR-elicited excitation of subicular neurons. Our results also demonstrate that activation of OXTRs excites subicular neurons by inhibiting a K^+ channel in ~25% of subicular neurons. This conclusion is based on the result that the I-V curve of the TGOT-elicited currents in one-fourth of the subicular neurons showed a reversal potential close to the K^+ reversal potential. Because depression of K^+ channels is involved in OXTR-mediated excitation in a small population of the subicular neurons, it is difficult to explore this mechanism further. Thus, the identity of the K^+ channels involved in OXTR-induced excitation of subicular neurons remains unresolved. In line with our results, another neuropeptide, gastrin-releasing peptide excites rat paraventricular thalamic neurons by simultaneous activation of TRPV1 channels and suppression of K^+ channels (Hermes et al. 2013).

Activation of OXTRs has been shown to increase neuronal excitability in different neurons by distinct ionic mechanisms including activation of cationic channels, suppression of K^+ channels, or both. For instance, OXTR activation induces membrane depolarization by inhibiting KCNQ-based M channels in CA2 pyramidal neurons of the hippocampus (Tirko et al. 2018) and the inwardly rectifying K^+ channels in the lateral nucleus of the central amygdala (Hu et al. 2020); OXTR activation up-modulates L-type Ca^{2+} channels to excite CA1 GABAergic interneurons in the hippocampus (Maniezzi et al. 2019). In the ventral tegmental area and interfascicular nucleus of mouse midbrain, OXT increases neuronal excitability by activating a nonselective cation channel and Na^+-Ca^{2+} exchanger (Tang et al. 2014); TRPC-like channels are targets of OXT-elicited excitation of tuberoinfundibular dopamine neurons (Briffaud et al. 2015); OXT also depolarizes substantia gelatinosa neurons of adult rat spinal cord by inhibiting a K^+ conductance and opening a cationic conductance (Jiang et al. 2014). In the present study, we further identified that TRPV1 channels are another target for OXTRs at least in neurons of the subiculum.

OXTRs are coupled to $G\alpha_q$ proteins, resulting in activation of PLCβ which hydrolyzes PIP_2 to generate IP_3 to increase intracellular Ca^{2+} release and DAG to activate PKC. Our results demonstrate that PLCβ is required for OXTR-mediated excitation of subicular neurons, while Ca^{2+} released from intracellular stores is unnecessary. Nevertheless, PKC and PLCβ-induced depletion of PIP_2 is involved in OXTR-induced excitation of subicular neurons. Because we demonstrated that activation of OXTRs excites subicular neurons primarily by activating TRPV1 channels, it is reasonable to conjecture that PLCβ, PKC, and PIP_2 interact with TRPV1 channels to excite subicular neurons. Consistent with this idea, many $G\alpha_q$-coupled receptors, including bradykinin receptor 2 (Shin et al. 2002), prostaglandin receptor (Moriyama et al. 2005), protease-activated receptor 2 (Amadesi et al. 2004), histamine receptor 1 (Shim et al. 2007), endothelin-1 receptors (Plant et al. 2007), neurokinin receptors (Zhang et al. 2007; Sculptoreanu et al. 2008), and sensory neuron-specific Mas-related G protein-coupled receptors-X1 (MRGPR-X1) (Solinski et al. 2012) are reported to activate TRPV1 channels. Multiple signaling mechanisms including DAG, PKC, and PIP_2 depletion have been proposed to explain the activation of TRPV1 channels by G protein-coupled receptors, as exemplified in the mechanism underlying MRGPR-X1-elicited activation of TRPV1 channels (Solinski et al. 2012). DAG has been reported to bind to and directly activate TRPV1 channels in rat dorsal root ganglion neurons (Woo et al. 2008); G protein-coupled receptors activate TRPV1 via PKC (Premkumar and Ahern 2000; Julius and Basbaum 2001; Plant et al. 2007; Kumar et al. 2017) and PKC-mediated phosphorylation of TRPV1 channels increases channel activity (Premkumar and Ahern 2000; Ahern 2003; Studer and McNaughton 2010); PLCβ-mediated depletion of PIP_2 relieves TRPV1 from the inhibition of PIP_2, thereby activating the ion channels (Chuang et al. 2001; Prescott and Julius 2003; Suh and Hille 2008). Although the role of DAG in the subiculum needs further exploration, our results demonstrate that PKC and PLCβ-mediated degradation of PIP_2 is involved in OXTR-elicited

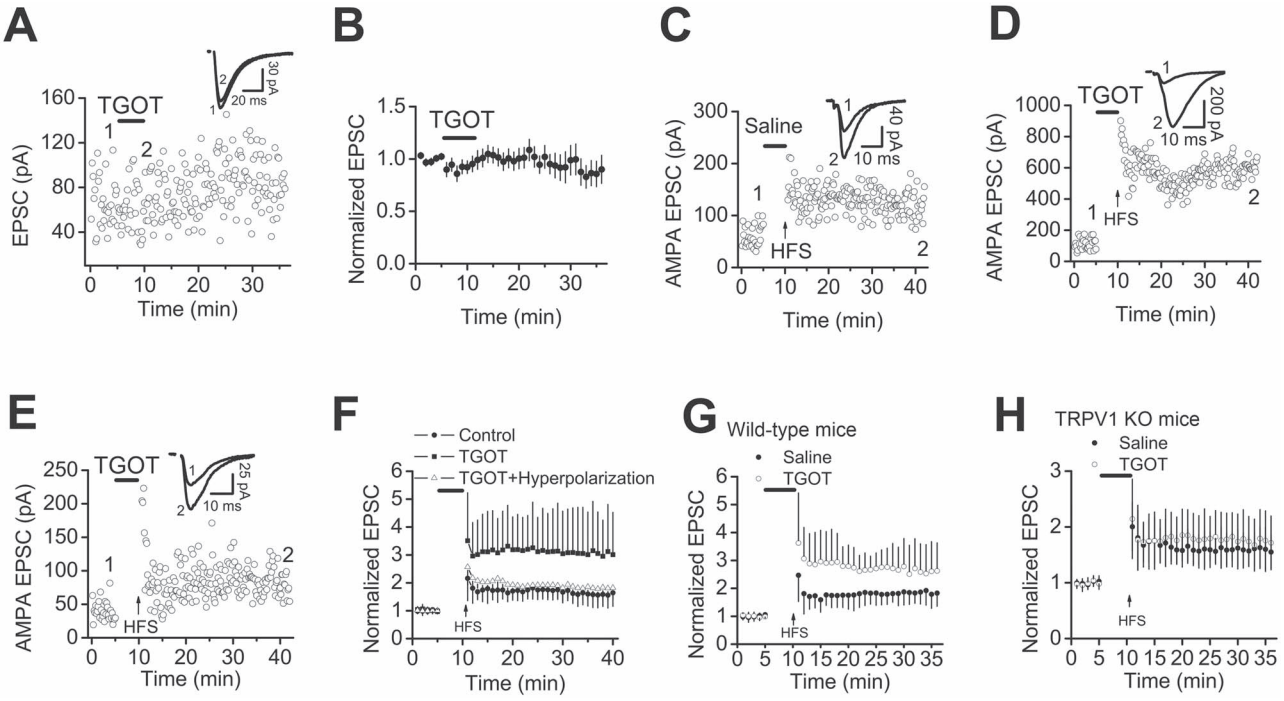

Figure 8. OXTR-elicited depolarization of subicular neurons facilitates LTP induction via activation of TRPV1 channels. (*A*) Scatter plot of the AMPA EPSCs recorded at a putative CA1-subiculum synapse in response to bath application of TGOT. Inset shows the AMPA EPSCs recorded at the time points indicated in the figure. (*B*) Averaged time course of the AMPA EPSCs before, during, and after the application of TGOT ($n = 8$). (*C*) Time course of LTP at a putative CA1-subiculum synapse elicited by HFS after bath perfusion of the extracellular solution containing saline (0.9% NaCl) for 5 min. Inset shows the AMPA EPSCs recorded at the time points indicated in the figure. (*D*) Time course of LTP at a putative CA1-subiculum synapse elicited by HFS during bath perfusion of the extracellular solution containing TGOT for 5 min. Inset shows the AMPA EPSCs recorded at the time points indicated in the figure. (*E*) Time course of LTP at a putative CA1-subiculum synapse in response to bath application of TGOT plus a negative current injection during the application of HFS protocol. (*F*) Averaged LTPs in response to bath application of saline, TGOT, or TGOT plus negative current injection during the application of HFS protocol. (*G*) Averaged LTP in response to bath application of saline or TGOT in slices cut from WT mice. (*F*) Averaged LTP in response to bath application of saline or TGOT in slices cut from TRPV1 KO mice.

excitation of subicular neurons. Furthermore, PKCα (Gu et al. 2018) and PKCε (Premkumar and Ahern 2000; Numazaki et al. 2002; Mandadi et al. 2006; Zhang et al. 2007) are involved in the activation of TRPV1 channels. PKCα is a conventional PKC which depends on both DAG and Ca^{2+} for function, whereas PKCε is a novel PKC which is Ca^{2+}-independent, but DAG-dependent. Whilst our result that application of BAPTA to lower intracellular Ca^{2+} level significantly reduced TGOT-induced depolarization could be explained by BAPTA-induced inactivation of the conventional PKC such as PKCα, it is also possible that intracellular Ca^{2+} could be required for other unidentified signaling molecules which are essential for the effects of TGOT. In this case, a role for PKCε cannot be excluded. Further experiments are required to identify the PKC isoform(s) involved in OXTR-elicited excitation of subicular neurons.

Whilst OXTR-mediated depolarization led to AP firing in about 52% of subicular neurons, demonstrating that activation of OXTRs increases neuronal network activity, the remaining 48% of cells showed only a subthreshold depolarization. We showed that OXTR-induced depolarization also facilitates LTP by activation of TRPV1 channels. Several mechanisms could be postulated to explain OXTR-elicited augmentation of LTP. First, NMDA receptors are involved in the induction of LTP at the CA1-subiculum synapses (Wozny et al. 2008). NMDA receptors are voltage-dependently blocked by Mg^{2+}. OXTR-induced depolarization likely facilitated NMDA receptor opening and thus augmented LTP. Second, TRPV1 channels are Ca^{2+}-permeant. OXTR-elicited activation of TRPV1 channels could increase intracellular Ca^{2+}, thereby enhancing LTP. Consistent with our results, activation of OXTRs enhances LTP in the CA1 region (Tomizawa et al. 2003; Lin et al. 2012) and activation of TRPV1 channels, the target of OXTRs, augments LTP as well. For instance, TRPV1 KO mice showed decreased LTP in the hippocampus (Marsch et al. 2007), whereas the application of TRPV1 agonists facilitates the induction of LTP (Li et al. 2008). While the mechanisms underlying TRPV1 channel-mediated facilitation of LTP in the CA1 region could be due to TRPV1 channel-elicited long-term depression of GABAergic transmission (Gibson et al. 2008; Bennion et al. 2011), the role of TRPV1 channels in OXTR-elicited augmentation of LTP in the subiculum is unlikely relevant to GABAergic transmission because our extracellular solution contained the $GABA_A$ receptor blocker, picrotoxin.

The subiculum is the major output pathway of hippocampus and targets a variety of cortical and subcortical areas (O'Mara et al. 2001). This divergent output makes the subiculum an integral component in networks underlying diverse functions and behaviors, such as regulation of spatial memory (O'Mara et al. 2001; O'Mara et al. 2009), the functions of hypothalamic–pituitary axis (O'Mara 2005) and stress responses (Mueller et al. 2004). Additionally, dysregulation of subiculum has been implicated in pathological conditions such as epilepsy (Stafstrom 2005; Wozny et al. 2005) and drug addiction (O'Mara et al. 2009). Oxytocinergic fibers project from the parvocellular neurons of

the hypothalamus to discrete extrahypothalamic limbic brain regions including the hippocampus, subiculum, amygdala, and nucleus accumbens (Buijs 1978; Lang et al. 1983; Hawthorn et al. 1985; Jurek and Neumann 2018). OXT is a neuromodulator that regulates a diverse range of functions including emotional responses (Neumann 2008; Viviani et al. 2011; Knobloch et al. 2012), social affiliation (Feldman 2012), grooming (Amico et al. 2004), sexual behaviors (Argiolas and Gessa 1991), social (Bielsky and Young 2004) and spatial (Tomizawa et al. 2003) memories, and may possess therapeutic potential for neuropsychiatric disorders, such as autism and schizophrenia (Zik and Roberts 2015). Many of these functions associated with OXT are related to the limbic structures including the subiculum. Because many structures in the limbic system are reciprocally connected, functional alteration of one component such as the subiculum would likely trigger the network activity in the limbic system. Consistent with this scenario, peripheral application of OXT activates the subiculum first in the brain (Ferris et al. 2015). Our results demonstrate that activation of OXTRs excites subicular neurons via PLCβ-, PKC- and PIP_2 depletion-mediated activation of TRPV1 channels and depression of K^+ channels. Knowing the molecular targets of OXTRs in the subiculum would facilitate the understanding of the functions of OXT in vivo. For example, activation of OXTRs modulates anxiety (Neumann 2008; Viviani et al. 2011; Knobloch et al. 2012). Because TRPV1 channels (Marsch et al. 2007; Ho et al. 2012), PLCβ (McOmish et al. 2008; Xiao et al. 2012), and PKC (Bowers et al. 2000; Lesscher et al. 2008; Liu et al. 2014) are involved in the modulation of anxiety, our results may provide an ionic and signaling mechanism to explain the modulatory effects of OXT in anxiety. Furthermore, OXT improves spatial memory (Tomizawa et al. 2003) which is closely associated with the subiculum. TRPV1 (Genro et al. 2012; Edwards 2014; Bannazadeh et al. 2017; Bashiri et al. 2018) and PKC (Van der Zee and Douma 1997) are involved in modulating memories. Our results, therefore, provide a cellular and molecular mechanism to explain the effects of OXT on memories as well.

Notes

Conflict of interest: The authors declares no conflict of interest.

Funding

This work was supported by the National Institute Of General Medical Sciences (NIGMS) and National Institute Of Mental Health (NIMH) grant R01MH118258 to S.L.

References

Ahern GP. 2003. Activation of TRPV1 by the satiety factor oleoylethanolamide. *J Biol Chem*. 278:30429–30434.

Amadesi S, Nie J, Vergnolle N, Cottrell GS, Grady EF, Trevisani M, Manni C, Geppetti P, McRoberts JA, Ennes H *et al*. 2004. Protease-activated receptor 2 sensitizes the capsaicin receptor transient receptor potential vanilloid receptor 1 to induce hyperalgesia. *J Neurosci*. 24:4300–4312.

Amico JA, Vollmer RR, Karam JR, Lee PR, Li X, Koenig JI, McCarthy MM. 2004. Centrally administered oxytocin elicits exaggerated grooming in oxytocin null mice. *Pharmacol Biochem Behav*. 78:333–339.

Argiolas A, Gessa GL. 1991. Central functions of oxytocin. *Neurosci Biobehav Rev*. 15:217–231.

Bannazadeh M, Fatehi F, Fatemi I, Roohbakhsh A, Allahtavakoli M, Nasiri M, Azin M, Shamsizadeh A. 2017. The role of transient receptor potential vanilloid type 1 in unimodal and multimodal object recognition task in rats. *Pharmacol Rep*. 69:526–531.

Bashiri H, Hosseini-Chegeni H, Alsadat Sharifi K, Sahebgharani M, Salari AA. 2018. Activation of TRPV1 receptors affects memory function and hippocampal TRPV1 and CREB mRNA expression in a rat model of biliary cirrhosis. *Neurol Res*. 40:938–947.

Bennion D, Jensen T, Walther C, Hamblin J, Wallmann A, Couch J, Blickenstaff J, Castle M, Dean L, Beckstead S *et al*. 2011. Transient receptor potential vanilloid 1 agonists modulate hippocampal CA1 LTP via the GABAergic system. *Neuropharmacology*. 61:730–738.

Bielsky IF, Young LJ. 2004. Oxytocin, vasopressin, and social recognition in mammals. *Peptides*. 25:1565–1574.

Birnbaumer M. 2000. Vasopressin receptors. *Trends Endocrinol Metab*. 11:406–410.

Bowers BJ, Collins AC, Tritto T, Wehner JM. 2000. Mice lacking PKC gamma exhibit decreased anxiety. *Behav Genet*. 30:111–121.

Briffaud V, Williams P, Courty J, Broberger C. 2015. Excitation of tuberoinfundibular dopamine neurons by oxytocin: crosstalk in the control of lactation. *J Neurosci*. 35:4229–4237.

Buijs RM. 1978. Intra- and extrahypothalamic vasopressin and oxytocin pathways in the rat. Pathways to the limbic system, medulla oblongata and spinal cord. *Cell Tissue Res*. 192:423–435.

Chuang HH, Prescott ED, Kong H, Shields S, Jordt SE, Basbaum AI, Chao MV, Julius D. 2001. Bradykinin and nerve growth factor release the capsaicin receptor from PtdIns(4,5)P2-mediated inhibition. *Nature*. 411:957–962.

Dreifuss JJ, Tribollet E, Dubois-Dauphin M, Raggenbass M. 1989. Neurohypophysial hormones: neuronal effects in autonomic and limbic areas of the rat brain. *Arch Histol Cytol*. 52(Suppl):129–138.

Dubrovsky B, Harris J, Gijsbers K, Tatarinov A. 2002. Oxytocin induces long-term depression on the rat dentate gyrus: possible ATPase and ectoprotein kinase mediation. *Brain Res Bull*. 58:141–147.

Edwards JG. 2014. TRPV1 in the central nervous system: synaptic plasticity, function, and pharmacological implications. *Prog Drug Res*. 68:77–104.

Feldman R. 2012. Oxytocin and social affiliation in humans. *Horm Behav*. 61:380–391.

Fenwick AJ, Fowler DK, Wu SW, Shaffer FJ, Lindberg JEM, Kinch DC, Peters JH. 2017. Direct anandamide activation of TRPV1 produces divergent calcium and current responses. *Front Mol Neurosci*. 10:200.

Ferris CF, Yee JR, Kenkel WM, Dumais KM, Moore K, Veenema AH, Kulkarni P, Perkybile AM, Carter CS. 2015. Distinct BOLD activation profiles following central and peripheral oxytocin administration in awake rats. *Front Behav Neurosci*. 9:245.

Freund-Mercier MJ, Stoeckel ME, Palacios JM, Pazos A, Reichhart JM, Porte A, Richard P. 1987. Pharmacological characteristics and anatomical distribution of [3H]oxytocin-binding sites in the Wistar rat brain studied by autoradiography. *Neuroscience*. 20:599–614.

Genro BP, de Oliveira Alvares L, Quillfeldt JA. 2012. Role of TRPV1 in consolidation of fear memories depends on the averseness of the conditioning procedure. *Neurobiol Learn Mem*. 97:355–360.

Gibson HE, Edwards JG, Page RS, Van Hook MJ, Kauer JA. 2008. TRPV1 channels mediate long-term depression at synapses on hippocampal interneurons. *Neuron*. 57:746–759.

Graves AR, Moore SJ, Bloss EB, Mensh BD, Kath WL, Spruston N. 2012. Hippocampal pyramidal neurons comprise two distinct cell types that are countermodulated by metabotropic receptors. *Neuron*. 76:776–789.

Greene JR, Mason A. 1996. Neuronal diversity in the subiculum: correlations with the effects of somatostatin on intrinsic properties and on GABA-mediated IPSPs in vitro. *J Neurophysiol*. 76:1657–1666.

Gu Y, Li G, Huang LYM. 2018. Inflammation induces Epac-protein kinase C alpha and epsilon signaling in TRPV1-mediated hyperalgesia. *Pain*. 159:2383–2393.

Harden SW, Frazier CJ. 2016. Oxytocin depolarizes fast-spiking hilar interneurons and induces GABA release onto mossy cells of the rat dentate gyrus. *Hippocampus*. 26:1124–1139.

Hawthorn J, Ang VT, Jenkins JS. 1985. Effects of lesions in the hypothalamic paraventricular, supraoptic and suprachiasmatic nuclei on vasopressin and oxytocin in rat brain and spinal cord. *Brain Res*. 346:51–57.

Hermes ML, Kolaj M, Coderre EM, Renaud LP. 2013. Gastrin-releasing peptide acts via postsynaptic BB2 receptors to modulate inward rectifier K+ and TRPV1-like conductances in rat paraventricular thalamic neurons. *J Physiol*. 591:1823–1839.

Ho KW, Ward NJ, Calkins DJ. 2012. TRPV1: a stress response protein in the central nervous system. *Am J Neurodegener Dis*. 1:1–14.

Hu B, Boyle CA, Lei S. 2020. Oxytocin receptors excite lateral nucleus of central amygdala by phospholipase Cbeta- and protein kinase C-dependent depression of inwardly rectifying K(+) channels. *J Physiol*. 598:3501–3520.

Hu B, Cilz NI, Lei S. 2017. Somatostatin depresses the excitability of subicular bursting cells: roles of inward rectifier K(+) channels, KCNQ channels and Epac. *Hippocampus*. 27: 971–984.

Jiang CY, Fujita T, Kumamoto E. 2014. Synaptic modulation and inward current produced by oxytocin in substantia gelatinosa neurons of adult rat spinal cord slices. *J Neurophysiol*. 111:991–1007.

Julius D, Basbaum AI. 2001. Molecular mechanisms of nociception. *Nature*. 413:203–210.

Jurek B, Neumann ID. 2018. The oxytocin receptor: from intracellular Signaling to behavior. *Physiol Rev*. 98:1805–1908.

Knobloch HS, Charlet A, Hoffmann LC, Eliava M, Khrulev S, Cetin AH, Osten P, Schwarz MK, Seeburg PH, Stoop R *et al*. 2012. Evoked axonal oxytocin release in the central amygdala attenuates fear response. *Neuron*. 73:553–566.

Kumar R, Hazan A, Geron M, Steinberg R, Livni L, Matzner H, Priel A. 2017. Activation of transient receptor potential vanilloid 1 by lipoxygenase metabolites depends on PKC phosphorylation. *FASEB J*. 31:1238–1247.

Lang RE, Heil J, Ganten D, Hermann K, Rascher W, Unger T. 1983. Effects of lesions in the paraventricular nucleus of the hypothalamus on vasopressin and oxytocin contents in brainstem and spinal cord of rat. *Brain Res*. 260:326–329.

Lesscher HM, McMahon T, Lasek AW, Chou WH, Connolly J, Kharazia V, Messing RO. 2008. Amygdala protein kinase C epsilon regulates corticotropin-releasing factor and anxiety-like behavior. *Genes Brain Behav*. 7:323–333.

Li HB, Mao RR, Zhang JC, Yang Y, Cao J, Xu L. 2008. Antistress effect of TRPV1 channel on synaptic plasticity and spatial memory. *Biol Psychiatry*. 64:286–292.

Lin YT, Huang CC, Hsu KS. 2012. Oxytocin promotes long-term potentiation by enhancing epidermal growth factor receptor-mediated local translation of protein kinase Mzeta. *J Neurosci*. 32:15476–15488.

Liu B, Feng J, Wang JH. 2014. Protein kinase C is essential for kainate-induced anxiety-related behavior and glutamatergic synapse upregulation in prelimbic cortex. *CNS Neurosci Ther*. 20:982–990.

Mandadi S, Tominaga T, Numazaki M, Murayama N, Saito N, Armati PJ, Roufogalis BD, Tominaga M. 2006. Increased sensitivity of desensitized TRPV1 by PMA occurs through PKCepsilon-mediated phosphorylation at S800. *Pain*. 123: 106–116.

Maniezzi C, Talpo F, Spaiardi P, Toselli M, Biella G. 2019. Oxytocin increases phasic and tonic GABAergic transmission in CA1 region of mouse hippocampus. *Front Cell Neurosci*. 13:178.

Marsch R, Foeller E, Rammes G, Bunck M, Kossl M, Holsboer F, Zieglgansberger W, Landgraf R, Lutz B, Wotjak CT. 2007. Reduced anxiety, conditioned fear, and hippocampal long-term potentiation in transient receptor potential vanilloid type 1 receptor-deficient mice. *J Neurosci*. 27:832–839.

Mason A. 1993. Electrophysiology and burst-firing of rat subicular pyramidal neurons in vitro: a comparison with area CA1. *Brain Res*. 600:174–178.

Mattia D, Hwa GG, Avoli M. 1993. Membrane properties of rat subicular neurons in vitro. *J Neurophysiol*. 70:1244–1248.

McOmish CE, Burrows EL, Howard M, Hannan AJ. 2008. PLC-beta1 knockout mice as a model of disrupted cortical development and plasticity: behavioral endophenotypes and dysregulation of RGS4 gene expression. *Hippocampus*. 18:824–834.

Melis MR, Argiolas A. 2011. Central control of penile erection: a re-visitation of the role of oxytocin and its interaction with dopamine and glutamic acid in male rats. *Neurosci Biobehav Rev*. 35:939–955.

Melis MR, Succu S, Cocco C, Caboni E, Sanna F, Boi A, Ferri GL, Argiolas A. 2010. Oxytocin induces penile erection when injected into the ventral subiculum: role of nitric oxide and glutamic acid. *Neuropharmacology*. 58:1153–1160.

Melis MR, Succu S, Sanna F, Boi A, Argiolas A. 2009. Oxytocin injected into the ventral subiculum or the posteromedial cortical nucleus of the amygdala induces penile erection and increases extracellular dopamine levels in the nucleus accumbens of male rats. *Eur J Neurosci*. 30:1349–1357.

Moriyama T, Higashi T, Togashi K, Iida T, Segi E, Sugimoto Y, Tominaga T, Narumiya S, Tominaga M. 2005. Sensitization of TRPV1 by EP1 and IP reveals peripheral nociceptive mechanism of prostaglandins. *Mol Pain*. 1:3.

Mueller NK, Dolgas CM, Herman JP. 2004. Stressor-selective role of the ventral subiculum in regulation of neuroendocrine stress responses. *Endocrinology*. 145:3763–3768.

Muhlethaler M, Charpak S, Dreifuss JJ. 1984. Contrasting effects of neurohypophysial peptides on pyramidal and non-pyramidal neurones in the rat hippocampus. *Brain Res*. 308:97–107.

Muhlethaler M, Dreifuss JJ. 1983. Excitation of hippocampal neurones by posterior pituitary peptides: vasopressin and oxytocin compared. *Prog Brain Res*. 60:147–151.

Muller C, Morales P, Reggio PH. 2018. Cannabinoid ligands targeting TRP channels. *Front Mol Neurosci*. 11:487.

Neumann ID. 2008. Brain oxytocin: a key regulator of emotional and social behaviours in both females and males. *J Neuroendocrinol*. 20:858–865.

Numazaki M, Tominaga T, Toyooka H, Tominaga M. 2002. Direct phosphorylation of capsaicin receptor VR1 by protein kinase Cepsilon and identification of two target serine residues. *J Biol Chem*. 277:13375–13378.

O'Mara S. 2005. The subiculum: what it does, what it might do, and what neuroanatomy has yet to tell us. *J Anat*. 207: 271–282.

O'Mara SM, Commins S, Anderson M, Gigg J. 2001. The subiculum: a review of form, physiology and function. *Prog Neurobiol*. 64:129–155.

O'Mara SM, Sanchez-Vives MV, Brotons-Mas JR, O'Hare E. 2009. Roles for the subiculum in spatial information processing, memory, motivation and the temporal control of behaviour. *Prog Neuropsychopharmacol Biol Psychiatry*. 33: 782–790.

Owen SF, Tuncdemir SN, Bader PL, Tirko NN, Fishell G, Tsien RW. 2013. Oxytocin enhances hippocampal spike transmission by modulating fast-spiking interneurons. *Nature*. 500: 458–462.

Pettibone DJ, Guidotti M, Harrell CM, Jasper JR, Lis EV, O'Brien JA, Reiss DR, Woyden CJ, Bock MG, Evans BE *et al*. 1995. Progress in the development of oxytocin antagonists for use in preterm labor. *Adv Exp Med Biol*. 395:601–612.

Plant TD, Zollner C, Kepura F, Mousa SS, Eichhorst J, Schaefer M, Furkert J, Stein C, Oksche A. 2007. Endothelin potentiates TRPV1 via ETA receptor-mediated activation of protein kinase C. *Mol Pain*. 3:35.

Premkumar LS, Ahern GP. 2000. Induction of vanilloid receptor channel activity by protein kinase C. *Nature*. 408: 985–990.

Prescott ED, Julius D. 2003. A modular PIP2 binding site as a determinant of capsaicin receptor sensitivity. *Science*. 300:1284–1288.

Rodriguez-Menchaca AA, Adney SK, Zhou L, Logothetis DE. 2012. Dual regulation of voltage-sensitive ion channels by PIP(2). *Front Pharmacol*. 3:170.

Sculptoreanu A, Aura Kullmann F, de Groat WC. 2008. Neurokinin 2 receptor-mediated activation of protein kinase C modulates capsaicin responses in DRG neurons from adult rats. *Eur J Neurosci*. 27:3171–3181.

Shim WS, Tak MH, Lee MH, Kim M, Kim M, Koo JY, Lee CH, Kim M, Oh U. 2007. TRPV1 mediates histamine-induced itching via the activation of phospholipase A2 and 12-lipoxygenase. *J Neurosci*. 27:2331–2337.

Shin J, Cho H, Hwang SW, Jung J, Shin CY, Lee SY, Kim SH, Lee MG, Choi YH, Kim J *et al*. 2002. Bradykinin-12-lipoxygenase-VR1 signaling pathway for inflammatory hyperalgesia. *Proc Natl Acad Sci USA*. 99:10150–10155.

Smart D, Gunthorpe MJ, Jerman JC, Nasir S, Gray J, Muir AI, Chambers JK, Randall AD, Davis JB. 2000. The endogenous lipid anandamide is a full agonist at the human vanilloid receptor (hVR1). *Br J Pharmacol*. 129:227–230.

Solinski HJ, Zierler S, Gudermann T, Breit A. 2012. Human sensory neuron-specific Mas-related G protein-coupled receptors-X1 sensitize and directly activate transient receptor potential cation channel V1 via distinct signaling pathways. *J Biol Chem*. 287:40956–40971.

Song Z, McCann KE, JKt MN, Larkin TE 2nd, Huhman KL, Albers HE. 2014. Oxytocin induces social communication by activating arginine-vasopressin V1a receptors and not oxytocin receptors. *Psychoneuroendocrinology*. 50:14–19.

Stafstrom CE. 2005. The role of the subiculum in epilepsy and epileptogenesis. *Epilepsy Curr*. 5:121–129.

Studer M, McNaughton PA. 2010. Modulation of single-channel properties of TRPV1 by phosphorylation. *J Physiol*. 588:3743–3756.

Succu S, Sanna F, Argiolas A, Melis MR. 2011. Oxytocin injected into the hippocampal ventral subiculum induces penile erection in male rats by increasing glutamatergic neurotransmission in the ventral tegmental area. *Neuropharmacology*. 61:181–188.

Suh BC, Hille B. 2008. PIP2 is a necessary cofactor for ion channel function: how and why? *Annu Rev Biophys*. 37:175–195.

Tang Y, Chen Z, Tao H, Li C, Zhang X, Tang A, Liu Y. 2014. Oxytocin activation of neurons in ventral tegmental area and interfascicular nucleus of mouse midbrain. *Neuropharmacology*. 77:277–284.

Tirko NN, Eyring KW, Carcea I, Mitre M, Chao MV, Froemke RC, Tsien RW. 2018. Oxytocin transforms firing mode of CA2 hippocampal neurons. *Neuron*. 100:593–608 e593.

Tomizawa K, Iga N, Lu YF, Moriwaki A, Matsushita M, Li ST, Miyamoto O, Itano T, Matsui H. 2003. Oxytocin improves long-lasting spatial memory during motherhood through MAP kinase cascade. *Nat Neurosci*. 6:384–390.

Van der Zee EA, Douma BR. 1997. Historical review of research on protein kinase C in learning and memory. *Prog Neuropsychopharmacol Biol Psychiatry*. 21:379–406.

Viviani D, Charlet A, van den Burg E, Robinet C, Hurni N, Abatis M, Magara F, Stoop R. 2011. Oxytocin selectively gates fear responses through distinct outputs from the central amygdala. *Science*. 333:104–107.

Vrachnis N, Malamas FM, Sifakis S, Deligeoroglou E, Iliodromiti Z. 2011. The oxytocin-oxytocin receptor system and its antagonists as tocolytic agents. *Int J Endocrinol*. 2011:350546.

Wei D, Lee D, Cox CD, Karsten CA, Penagarikano O, Geschwind DH, Gall CM, Piomelli D. 2015. Endocannabinoid signaling mediates oxytocin-driven social reward. *Proc Natl Acad Sci USA*. 112:14084–14089.

Woo DH, Jung SJ, Zhu MH, Park CK, Kim YH, Oh SB, Lee CJ. 2008. Direct activation of transient receptor potential vanilloid 1(TRPV1) by diacylglycerol (DAG). *Mol Pain*. 4:42.

Wozny C, Knopp A, Lehmann TN, Heinemann U, Behr J. 2005. The subiculum: a potential site of ictogenesis in human temporal lobe epilepsy. *Epilepsia*. 46(Suppl 5):17–21.

Wozny C, Maier N, Schmitz D, Behr J. 2008. Two different forms of long-term potentiation at CA1-subiculum synapses. *J Physiol*. 586:2725–2734.

Wu LJ, Sweet TB, Clapham DE. 2010. International Union of Basic and Clinical Pharmacology. LXXVI. Current progress in the mammalian TRP ion channel family. *Pharmacol Rev*. 62:381–404.

Xiao Z, Jaiswal MK, Deng PY, Matsui T, Shin HS, Porter JE, Lei S. 2012. Requirement of phospholipase C and protein kinase C in cholecystokinin-mediated facilitation of NMDA channel function and anxiety-like behavior. *Hippocampus*. 22:1438–1450.

Zaninetti M, Raggenbass M. 2000. Oxytocin receptor agonists enhance inhibitory synaptic transmission in the rat hippocampus by activating interneurons in stratum pyramidale. *Eur J Neurosci*. 12:3975–3984.

Zhang H, Cang CL, Kawasaki Y, Liang LL, Zhang YQ, Ji RR, Zhao ZQ. 2007. Neurokinin-1 receptor enhances TRPV1 activity in primary sensory neurons via PKCepsilon: a novel pathway for heat hyperalgesia. *J Neurosci*. 27:12067–12077.

Zik JB, Roberts DL. 2015. The many faces of oxytocin: implications for psychiatry. *Psychiatry Res*. 226:31–37.